Volume-dependent ATP-conductive Large-Conductance Anion Channel as a Pathway for Swelling-induced ATP Release

Ravshan Z. Sabirov,[1,2] Amal K. Dutta,[1,2] and Yasunobu Okada[1,2]

[1]Department of Cell Physiology, National Institute for Physiological Sciences, Okazaki 444-8585, Japan
[2]Core Research for Evolutional Science and Technology of Japan Science and Technology Corporation, Okazaki 444-8585, Japan

ABSTRACT In mouse mammary C127i cells, during whole-cell clamp, osmotic cell swelling activated an anion channel current, when the phloretin-sensitive, volume-activated outwardly rectifying Cl^- channel was eliminated. This current exhibited time-dependent inactivation at positive and negative voltages greater than around ±25 mV. The whole-cell current was selective for anions and sensitive to Gd^{3+}. In on-cell patches, single-channel events appeared with a lag period of ~15 min after a hypotonic challenge. Under isotonic conditions, cell-attached patches were silent, but patch excision led to activation of currents that consisted of multiple large-conductance unitary steps. The current displayed voltage- and time-dependent inactivation similar to that of whole-cell current. Voltage-dependent activation profile was bell-shaped with the maximum open probability at −20 to 0 mV. The channel in inside-out patches had the unitary conductance of ~400 pS, a linear current-voltage relationship, and anion selectivity. The outward (but not inward) single-channel conductance was suppressed by extracellular ATP with an IC_{50} of 12.3 mM and an electric distance (δ) of 0.47, whereas the inward (but not outward) conductance was inhibited by intracellular ATP with an IC_{50} of 12.9 mM and δ of 0.40. Despite the open channel block by ATP, the channel was ATP-conductive with P_{ATP}/P_{Cl} of 0.09. The single-channel activity was sensitive to Gd^{3+}, SITS, and NPPB, but insensitive to phloretin, niflumic acid, and glibenclamide. The same pharmacological pattern was found in swelling-induced ATP release. Thus, it is concluded that the volume- and voltage-dependent ATP-conductive large-conductance anion channel serves as a conductive pathway for the swelling-induced ATP release in C127i cells.

KEY WORDS: ATP-conducting channel • maxi chloride channel • osmotic cell swelling • volume regulation

INTRODUCTION

Osmotic cell swelling is known to induce ATP release from a variety of cell types (Wang et al., 1996; Roman et al., 1997, 1999; Feranchak et al., 1998; Hazama et al., 1998b, 1999, 2000a,b; Mitchell et al.; 1998; Taylor et al., 1998; Light et al., 1999; Musante et al., 1999). In a wide variety of cell types, cell swelling activates volume-sensitive outwardly rectifying (VSOR)* intermediate-conductance anion channels, which exhibit significant permeability to large organic anions (Strange et al., 1996; Nilius et al., 1997; Okada, 1997). Therefore, the possibility exists that the VSOR anion channel serves as a pathway for swelling-induced release of anionic ATP. However, this prospect is at variance with the following observations. First, in human Intestine 407, mouse mammary C127/CFTR and bovine ciliary epithelial cells, swelling-induced ATP release was not inhibited by a number of blockers of VSOR anion channels, such as glibenclamide (Hazama et al., 1998b, 1999, 2000b; Mitchell et al., 1998), DPC (Mitchell et al., 1998), DIDS (Mitchell et al., 1998), SITS (Hazama et al., 1999), and arachidonic acid (Hazama et al., 1999). Second, Gd^{3+}, which is an effective blocker of swelling-induced ATP release (Taylor et al., 1998; Hazama et al., 1999, 2000b), did not inhibit VSOR anion currents in Intestine 407 (Hazama et al., 1999) and C127/CFTR cells (Hazama et al., 2000b). Third, mAbs, which block swelling-induced ATP release from Intestine 407 cells (Hazama et al., 1999), also failed to affect swelling-induced activation of anion currents in Intestine 407 (Hazama et al., 1999) and C127/CFTR cells (Hazama et al., 2000a). Fourth, heterologous expression of CFTR was shown to downregulate VSOR anion channel activity in CPAE and COS cells (Vennekens et al., 1999), whereas it upregulated swelling-induced ATP release from C127/CFTR cells (Hazama et al., 1998b, 2000b) or the presence of CFTR was required for swelling-induced ATP release from airway epithelial cells (Taylor et al., 1998).

Although it was previously proposed that CFTR serves as a conductive pathway for ATP release (Reisin et al., 1994; Schwiebert et al., 1995; Prat et al., 1996; Cantiello et al., 1997, 1998; Jiang et al., 1998; Lader et al., 2000), this "CFTR = ATP channel hypothesis" has been chal-

Address correspondence to Yasunobu Okada, Department of Cell Physiology, National Institute for Physiological Sciences, Myodaiji, Okazaki 444-8585, Japan. Fax: 81-564-55-7735; E-mail: okada@nips.ac.jp

Abbreviations used in this paper: VDAC, voltage-dependent anion channel; VDACL, voltage-dependent ATP-conductive large-conductance; VSOR, volume-sensitive outwardly rectifying.

lenged in a number of other studies (Takahashi et al., 1994; Li et al., 1996; Grygorczyk et al., 1996; Reddy et al., 1996; Grygorczyk and Hanrahan, 1997; Mitchell et al., 1998; Sugita et al., 1998; Watt et al., 1998). We also have provided several lines of evidence against this hypothesis for swelling-induced ATP release (Hazama et al., 1999, 2000b). First, ATP release was found to be induced by osmotic swelling in CFTR-lacking Intestine 407 and C127i cells. Second, a CFTR Cl^- channel blocker, glibenclamide, failed to inhibit swelling-induced ATP release in C127/CFTR cells. Third, a blocker of swelling-induced ATP release, Gd^{3+}, failed to affect cAMP-induced activation of CFTR Cl^- currents in C127/CFTR cells. Fourth, CFTR Cl^- currents were not affected by mAbs, which were found to abolish swelling-induced ATP release, in C127/CFTR cells.

In the present study, we searched for an alternative candidate anion channel that exhibits ATP conductivity and Gd^{3+} sensitivity in mouse mammary C127i cells. The volume- and voltage-dependent ATP-conductive large-conductance (VDACL) anion channel was found to exist in the plasma membrane and to share the same pharmacological profiles and CFTR-dependent modulation with swelling-induced ATP release.

MATERIALS AND METHODS

Cells

A cell line of mouse mammary tissue origin, C127i, was obtained from the American Type Culture Collection and grown in Dulbecco's modified Eagle's medium containing 10% FCS. A stable transfectant of C127i with the cDNA for human CFTR (C127/CFTR) was a gift from Dr. M.J. Welsh (University of Iowa), and was cultured in DMEM with 10% FCS and 200 μg ml^{-1} geneticin.

Solutions

The standard Ringer's solution contained the following (in mM): 135 NaCl, 5 KCl, 2 $CaCl_2$, 1 $MgCl_2$, 5 Na-HEPES, 6 HEPES, and 5 glucose, pH 7.4 (290 mosmol kg^{-1} H_2O). The hypotonic solution was made by reducing the concentration of NaCl in Ringer's solution to 100 mM (210 mosmol kg^{-1} H_2O). For selectivity measurements of whole-cell currents, 100 mM NaCl in Ringer's solution was replaced with 100 mM TEA-Cl or sodium glutamate. For single-channel selectivity measurements, 135 mM NaCl in Ringer's solution was replaced with 135 mM of TEA-Cl or Na salts of the anion that was being tested. For cation-to-anion selectivity measurements, NaCl concentration in Ringer's solution was lowered by isosmotic replacement with mannitol. For phosphate permeability measurements, 70 mM Na_2HPO_4 solution with pH 7.4 adjusted with HCl (calculated Cl^- concentration: 11 mM) was used. For the experiments under Ca^{2+}- and Mg^{2+}-free conditions, $CaCl_2$ and $MgCl_2$ were removed from, and 1 mM EDTA was added to, Ringer's solution.

The pipette solution for whole-cell experiments contained the following (in mM): 125 CsCl, 2 $CaCl_2$, 1 $MgCl_2$, 5 HEPES, and 10 EGTA, pH 7.4 (adjusted with CsOH; 275 mosmol kg^{-1} H_2O). In some whole-cell experiments, 1–5 mM ATP was added in the pipette solution. Pipette solution for cell-attached and inside-out experiments was standard Ringer's solution. When indicated, Cs-pipette and TEA-pipette solutions were used in which all monovalent cations were replaced with either Cs^+ or TEA^+. The pipette solution for outside-out experiments contained the following (in mM): 120 NaCl, 5 KCl, 2 $CaCl_2$, 1 $MgCl_2$, 5 HEPES, pH 7.4 (adjusted with NaOH), and 10 EGTA (pCa 7.7; 275 mosmol kg^{-1} H_2O).

For experiments testing the effect of ATP on channel activity, 2.5–25 mM Na_2ATP was added to the Ringer's bathing solution, and pH was adjusted to 7.4 with NaOH. For ATP-permeability measurements, 100 mM Na_2ATP solution was used after pH was adjusted at 7.4 with NaOH. All ATP-containing solutions were kept on ice and warmed to room temperature immediately before the experiment.

$GdCl_3$ was stored as a 30-mM stock solution in water and added directly to Ringer's solution immediately before the experiment. 5-Nitro-2-(phenylpropylamino)-benzoate (NPPB), glibenclamide, phloretin, 4-acetamido-4'-isothiocyanostilbene (SITS), niflumic acid (all from Sigma-Aldrich) were added to Ringer's solution immediately before use from stock solutions in DMSO to the final concentrations as indicated. The final DMSO concentration did not exceed 0.1% and DMSO did not have any effects, when added alone.

The osmolality of all solutions was measured using a freezing-point depression osmometer (model OM802; Vogel) or a vapor pressure osmometer (model Vapro 5520; Wescor).

Electrophysiology

Patch electrodes were fabricated from borosilicate glass using a micropipette puller (model P-97; Sutter Instrument Co.) and had a tip resistance of ~2 MΩ for whole-cell measurements and 2–8 MΩ for macro-patch and single-channel recordings when filled with pipette solution. Membrane currents were measured with an Axopatch 200A patch-clamp amplifier coupled to a Digi-Data 1200 interface (Axon Instruments) or an EPC-9 patch-clamp system (Heka-Electronics). The membrane potential was controlled by shifting the pipette potential (Vp). For whole-cell recordings, access resistance did not exceed 4 MΩ and was always compensated (to 70–80%). Whole-cell capacitance was 17.5 ± 1.4 pF ($n = 23$) and ranged from 9 to 32 pF. If not indicated, currents were filtered at 1 kHz and sampled at 2–5 kHz. Instantaneous currents for whole-cell and macro-patch recordings were measured 5–10 ms after the onset of the test pulses. Data acquisition and analysis were done using Pulse+PulseFit (Heka-Electronics) or pCLAMP6 (Axon Instruments) and WinASCD software (provided by Dr. G. Droogmans, Katholieke Universiteit Leuven, Belgium). Whenever bath Cl^- concentration was altered, a salt bridge containing 2 M KCl in 2% agarose was used to minimize bath electrode potential variations. Liquid junction potentials were measured by a separate patch electrode filled with 3 M KCl or calculated using pCLAMP8 algorithms, and both were found to be essentially the same (within 1–3 mV). The data were corrected for liquid junction potentials either on- or offline. All experiments were performed at room temperature (20–25°C).

Luciferin-Luciferase ATP Assay

Bulk extracellular ATP concentration was measured by the luciferin-luciferase assay (ATP luminescence kit; model AF-2L1; DKK-TOA Co.) at room temperature with an ATP analyzer (model AF-100; DKK-TOA Co.), as described previously (Hazama et al. 1999, 2000b). Briefly, C127i cells were cultured to confluence in 48-well plates. Culture medium was totally replaced with isotonic PBS solution (300 μl) containing the following (in mM): 137 NaCl, 2.7 KCl, 1 $CaCl_2$, 1 $MgCl_2$, 8.1 Na_2HPO_4, and 1.5 KH_2PO_4, pH 7.4 (300 mosmol kg^{-1} H_2O). Cells were incubated for 60 min at 37°C, and 100 μl of isotonic extracellular solution was removed and used as a control sample for background ATP release. A hypotonic challenge was then applied by gently adding

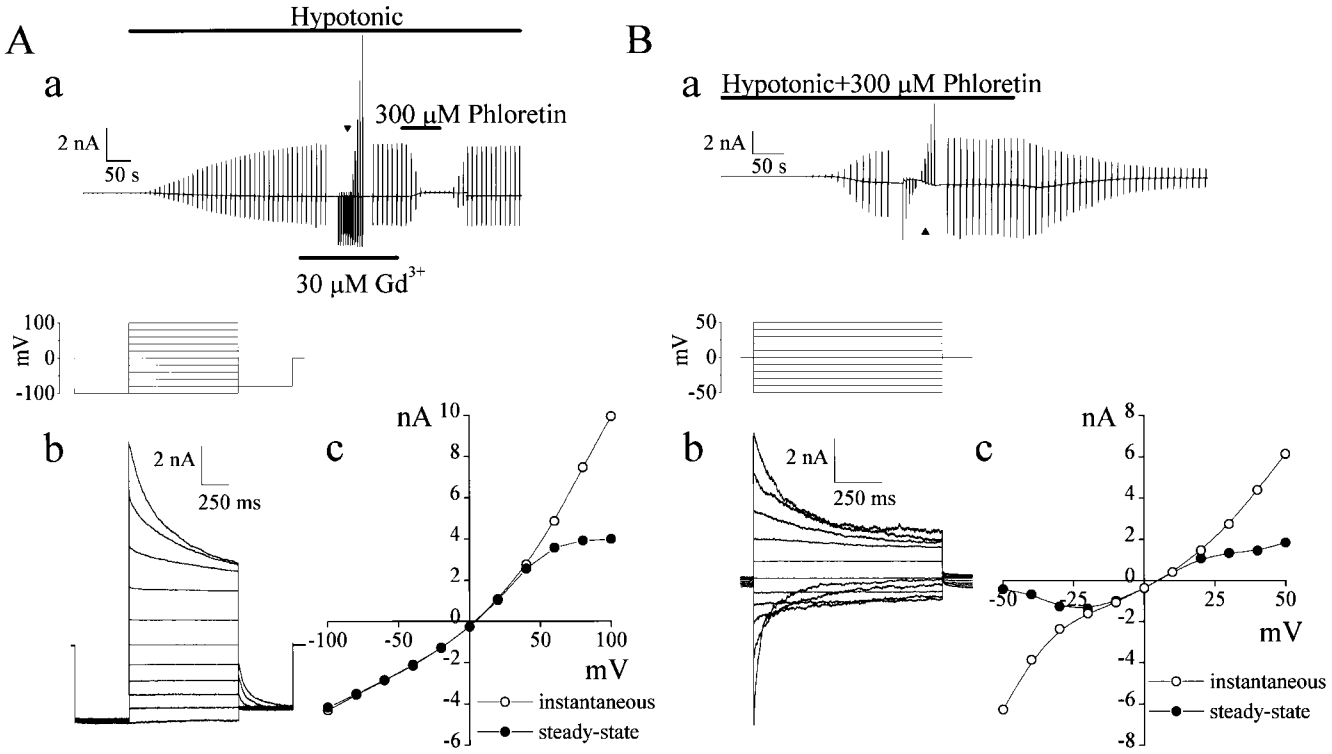

FIGURE 1. Two different types of whole-cell currents induced by osmotic swelling. (A) VSOR Cl^- currents recorded from a C127i cell dialyzed with pipette solution containing 5 mM ATP. (a) Representative record during application of alternating pulses from 0 to ±50 mV (every 10 s) or of step pulses from −100 to +100 mV in 20-mV increments at the arrowhead (protocol is shown in the inset). Horizontal bars indicate times during the application of hypotonic solution, and with the addition of 30 μM Gd^{3+} and 300 μM phloretin. (b) Expanded traces of current responses (at arrowhead in a) to step pulses. (c) Instantaneous and steady-state current-voltage relationships measured at the beginning (open circles) and the end (closed circles) of pulses, respectively. (B) Swelling-activated currents recorded from a C127i cell dialyzed with ATP-free pipette solution in the presence of extracellular phloretin (300 μM). (a) Representative record during application of alternating pulses from 0 to ±25 mV (every 10 s) or of step pulses from −50 to +50 mV in 10-mV increments at the arrowhead (protocol is shown in the inset). Horizontal bar indicates times of application of hypotonic solution containing 300 μM phloretin. (b) Expanded traces of current responses (at arrowhead in a) to step pulses. (c) Instantaneous and steady-state I-V relationships measured at the beginning (open circles) and the end (closed circles) of pulses, respectively.

100 or 200 μl of a solution with the following composition (in mM): 5 KCl, 1 $CaCl_2$, 1 $MgCl_2$, and 10 HEPES-NaOH, pH 7.4 (35 mosmol kg^{-1} H_2O) to the remaining 200 μl of isotonic solution to yield 71 or 56% hypotonicity, respectively. Preliminary studies showed that peak ATP release was observed after incubation for ~15 min in hypotonic solution. Thus, the cells were incubated for 15 min at either 25 or 37°C, and an extracellular solution sample (100 μl) was collected for the luminometric ATP assay of swelling-induced ATP release. When required, drugs were added to the hypotonic solution to give the final concentrations as indicated.

Data Analysis

Single-channel amplitudes were measured by manually placing cursors at the open and closed channel levels. By dividing a mean macro-patch current by a single-channel amplitude, the mean number of channels open, $P_o \cdot n$, was calculated, where P_o and n represent the open channel probability and the number of active channels, respectively. Dose–response data for ATP block of single channel amplitudes were fitted to the equation:

$$i = i_o/\{1 + ([A]/K_d)\}, \quad (1)$$

where i_o is the single-channel amplitude in the absence of ATP, i is the single-channel amplitude in the presence of ATP at a given concentration $[A]$, and K_d is the apparent dissociation constant.

The voltage dependence of blockade was examined using the Boltzmann equation:

$$i/i_o = (a + (1 - a)/\{1 + \exp[-z\delta F(V - V_o)/RT]\}), \quad (2)$$

where i_o is the single-channel current amplitude in the absence of ATP, i is the single-channel current amplitude in the presence of 25 mM ATP, δ is the fractional electrical distance from either extracellular or intracellular side, z is the valence of the blocker ($z = -4$ for ATP), V_o is a potential for half-maximal block, a is a limiting fractional current at high voltages, and F, R, and T have their usual thermodynamic meanings.

Permeability ratios for different anions (X) were calculated from Goldman-Hodgkin-Katz (GHK) equation:

$$\Delta E_{rev} = -RT/F \ln[(P_{Cl}[Cl]_o)/(P_{Cl}[Cl]_i + P_X[X])], \quad (3)$$

where ΔE_{rev} is the reversal potential in the presence of a test anion at a concentration $[X]$, $[Cl]_o$ is the Cl^- concentration in the pipette (standard Ringer's) solution, and $[Cl]_i$ is the Cl^- concentra-

tion in low Cl^- bath solutions containing different test anions. P_{Cl} and P_X are the permeabilities of Cl^- and test anion, respectively.

Na^+ to Cl^- permeability was calculated according to the Eq. 4:

$$\Delta E_{rev} = -RT/F \ln[(P_{Na}\gamma_{Na}[Na]_i + P_{Cl}\gamma_{Cl}[Cl]_o)/ (P_{Na}\gamma_{Na}[Na]_o + P_{Cl}\gamma_{Cl}[Cl]_i)], \quad (4)$$

where P_{Na} is the sodium permeability, $[Na]_i$ and $[Na]_o$ are intracellular and extracellular Na^+ concentrations, and γ_{Na} and γ_{Cl} are the activity coefficients of Na^+ and Cl^- (Harned and Owen, 1958).

Permeability ratio for polyvalent anions (*A*: phosphate and ATP) was calculated from GHK equation:

$$P_A/P_{Cl} = \{z_{Cl}^2[[Cl]_o - [Cl]_i \exp(\alpha z_{Cl} E_{rev})][1 - \exp(\alpha z_A E_{rev})]\}/ \{z_A^2[A]_i \exp(\alpha z_A E_{rev})[1 - \exp(\alpha z_{Cl} E_{rev})]\}, \quad (5)$$

where $\alpha = F/RT$; z_A and z_{Cl} are valences of the anion and Cl^-, respectively; $[Cl]_o$ and $[Cl]_i$ are the Cl^- concentrations in the pipette and in the bath, respectively; $[A]_i$ is the polyvalent anion concentration in the bath; and E_{rev} is the reversal potential. When no Cl^- was present in the bath, and therefore $[Cl]_i = 0$, the equation turns to the one used in Cantiello et al. (1997). z_A was assumed to be -2 for phosphate and -4 for ATP.

Data were analyzed in Origin 5.0 (MicroCal Software, Inc.). Pooled data are given as means ± SEM of observations (n). Statistical differences of the data were evaluated by paired or unpaired t test and considered at $P < 0.05$.

RESULTS

Gd^{3+}-sensitive Whole-Cell Anion Conductance Induced by Cell Swelling

Consistent with previous observations (Hazama et al., 2000b), C127i cells responded with activation of volume-sensitive outwardly rectifying (VSOR) Cl^- currents during swelling induced by a hypotonic challenge (74%) under whole-cell patch clamp using pipette solution containing ATP (Fig. 1 A). This current was Gd^{3+}-insensitive (Fig. 1 A, a) and exhibited inactivation at positive potentials larger than +40 mV (Fig. 1 A, b) as well as outward rectification (Fig. 1 A, c).

In searching for possible ATP-conductive pathways, we modified the whole-cell patch-clamp experiments to eliminate VSOR Cl^- currents in two ways: (1) by using a relatively selective blocker of VSOR channels, phloretin (Fan et al., 2001; Fig. 1 A, a); and (2) by excluding ATP from the pipette solution, since ATP is required for maintenance of VSOR channels activity (Okada, 1997). When C127i cells were exposed to hypotonic solution in the presence of 300 μM phloretin, cell swelling slowly and reversibly activated a current that had biophysical properties different from the VSOR Cl^- current (Fig. 1 B, a). This current displayed voltage-dependent inactivation, not only at positive potentials over +20 mV, but also at negative potentials below −30 mV (Fig. 1 B, b and c). Instantaneous I-V relationship was nonlinear, with outward and inward rectification at positive and negative potentials, respectively (Fig. 1 B, c).

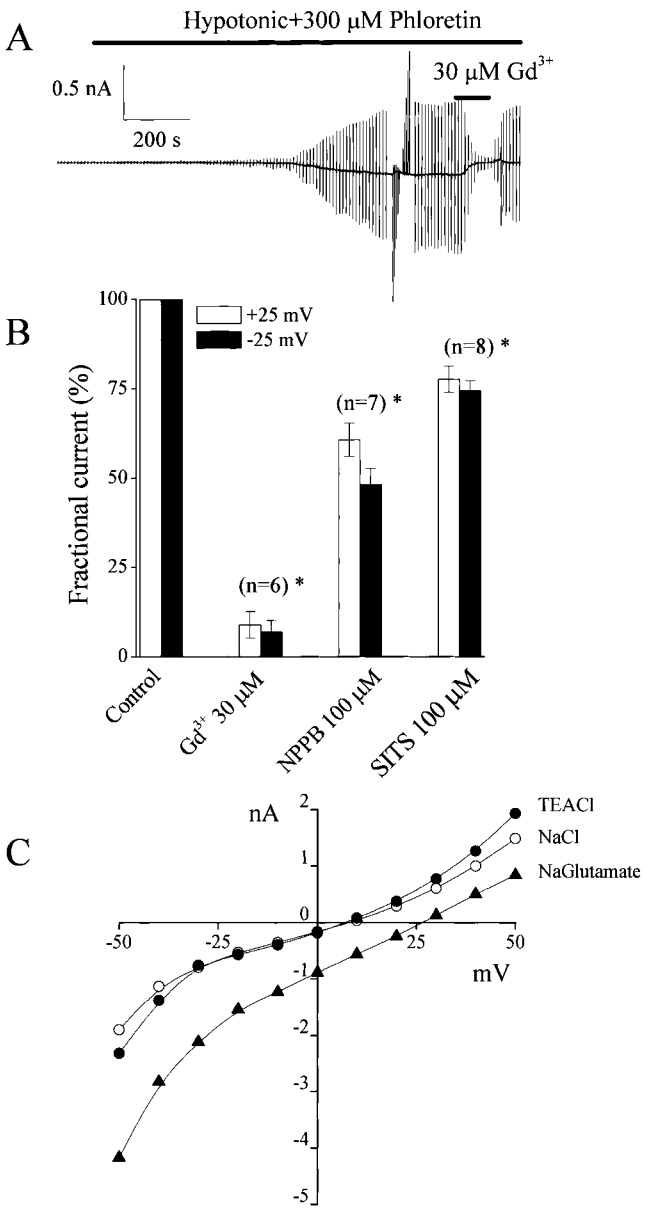

FIGURE 2. Gd^{3+} sensitivity and anion selectivity of swelling-induced phloretin-insensitive whole-cell currents. (A) Representative trace of Gd^{3+} sensitivity of currents recorded from a C127i cell dialyzed with ATP-free pipette solution during application of alternating pulses from 0 to ±25 mV or of step pulses from −50 to +50 mV in 10-mV increments. (B) Effects of Gd^{3+} (30 μM), NPPB (100 μM), and SITS (100 μM) on the instantaneous currents recorded upon application of step pulses of ±25 mV. All currents measured in the presence of these drugs were normalized to the respective currents measured before drug application. Also, currents were corrected for background currents. The SEM values are shown by vertical bars. (C) Representative instantaneous current-voltage relationships demonstrating the anion selectivity of this channel. All currents were recorded from a C127i cell exposed to a hypotonic solution containing 300 μM phloretin and 100 mM NaCl (open circles) or TEA-Cl (closed circles) or sodium gluconate (closed triangles). Similar data were obtained in five cells.

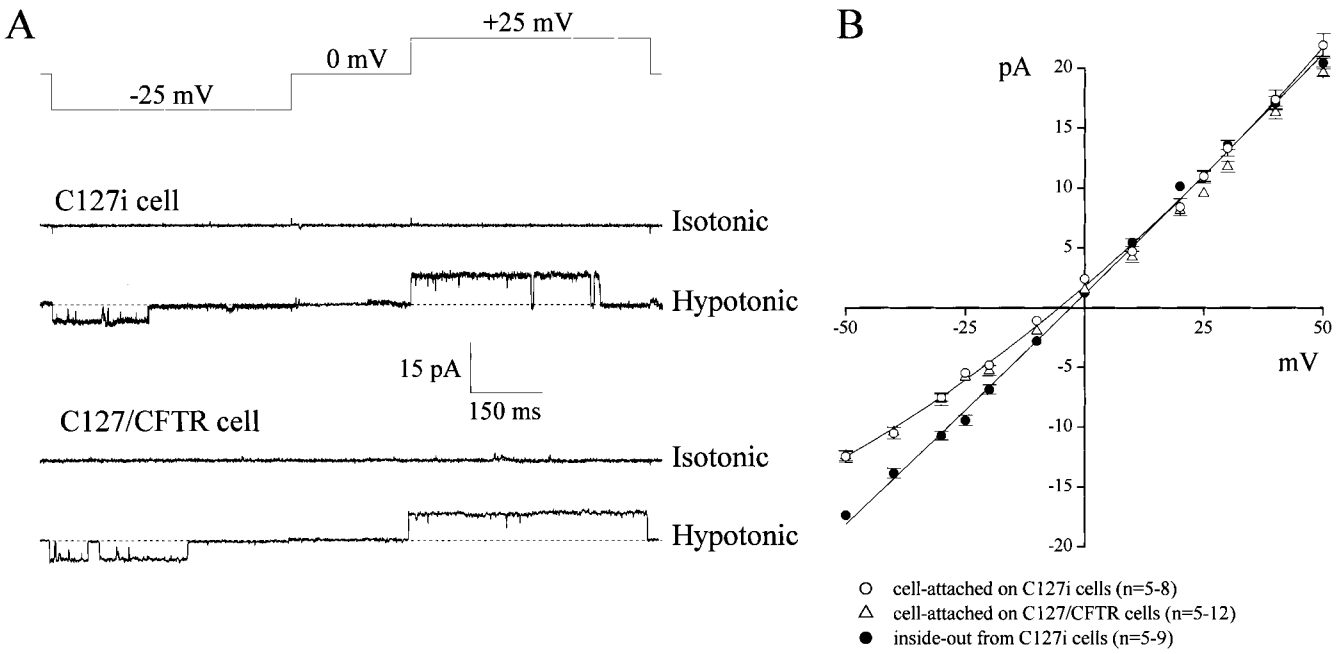

FIGURE 3. Swelling-induced activation of large-conductance single-channel currents in on-cell patches. (A) Representative current traces recorded under isotonic and hypotonic conditions on C127i (top traces) and C127/CFTR (bottom traces) cells, during application of alternating pulses from 0 to ±25 mV (protocol is shown at the top of the traces). (B) Unitary i-V relationships recorded in cell-attached patches on C127i (open circles) and C127/CFTR cells (open triangles) as well as in inside-out patches excised from C127i cells (closed circles). The SEM values are shown by vertical bars where the values exceed the symbol size.

Also, the steady-state current exhibited a negative slope resistance at potentials greater than around ±25 mV.

Steady-state current amplitude varied widely ranging from 240 pA up to 3,800 pA at +25 mV. Mean current density was 153 ± 54 pA/pF at +25 mV and −181 ± 56 pA/pF at −25 mV (n = 9). There was a delay of 3–20 min (mean 12.0 ± 1.2 min, n = 16) between hypotonic stimulation and current activation.

The phloretin-insensitive whole-cell current could be reversibly inhibited by 30 μM Gd^{3+} (Fig. 2 A). Whole-cell currents were also sensitive to 100 μM NPPB and SITS, however, those agents were less effective than 30 μM Gd^{3+}, as summarized in Fig. 2 B. Niflumic acid failed to affect whole-cell currents at a concentration of 200 μM (data not shown, n = 5). Also, replacing Na^+ ions with TEA^+ had no appreciable effect on the I-V relationship (Fig. 2 C) and voltage-dependent inactivation (data not shown). However, when 100 mM Cl^- in the hypotonic bath solution was replaced with 100 mM glutamate, the reversal potential was shifted by 23 ± 2 mV (n = 5) (Fig. 2 C), indicating anion selectivity of this swelling-induced phloretin-insensitive current.

Swelling-induced Large-Conductance Single-channel Activity in Cell-attached Patches

Single-channel events were rarely observed in cell-attached patches on C127i and C127/CFTR cells bathed in isotonic Ringer's solution (Fig. 3 A). When C127i cells were exposed to hypotonic solution with maintaining giga-sealed cell-attached patches, single-channel currents with a large conductance were observed (Fig. 3 A, middle trace) after a lag period of 15.0 ± 3.0 min (n = 10). This channel had a single-channel amplitude of 10.2 ± 0.3 pA (n = 12) and −5.7 ± 0.2 pA (n = 13) at +25 mV and −25 mV of −Vp, respectively. The unitary i-V relationship was slightly outwardly rectifying (presumably due to a lower Cl^- concentration within the cell) with a slope conductance of 402 ± 18 pS at positive voltages and 285 ± 15 pS at negative voltages, and the reversal potential was around −5 mV (Fig. 3 B, open circles). After excision, the i-V relationship became linear (Fig. 3 B, closed circles).

Channels with the same amplitude (Fig. 3 A, bottom trace) and i-V relation (Fig. 3 B, open triangles) were also observed in the cell-attached patches on C127/CFTR cells after exposure to hypotonic solution with a lag time of 4.4 ± 1.1 min (n = 10), which is significantly shorter than that in C127i cells ($P < 0.01$).

Even though we did not use the VSOR Cl^- channel blocker, phloretin, during single-channel recordings, we never detected VSOR Cl^- channel activity, which has an intermediate unitary conductance of 50–70 pS and profound outward rectification (Okada, 1997) in cell-attached patches. Single VSOR Cl^- channels were found only when preswollen cells were subjected to cell-attached patch clamp (data not shown, n = 11), but not when C127i cells were swelled after patch formation. These

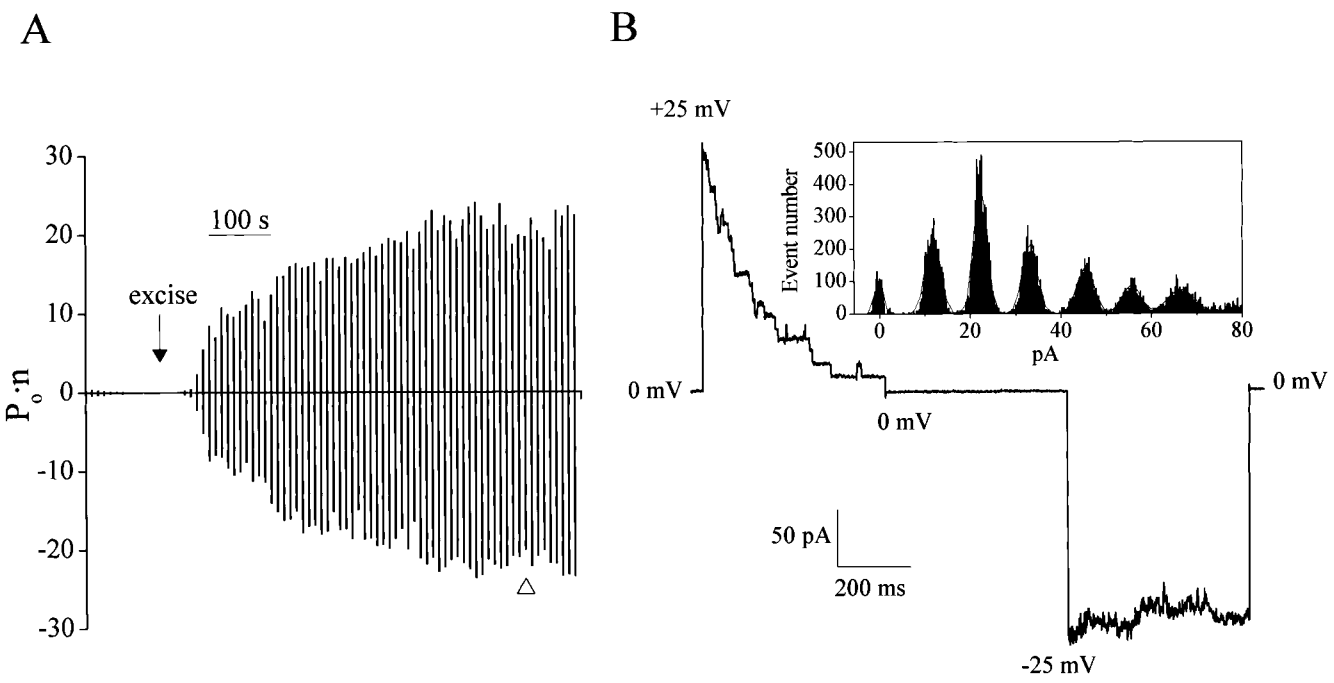

FIGURE 4. Excision-induced activation and voltage-dependent inactivation of large-conductance single-channel currents. (A) Time course of $P_o \cdot n$ recorded from a C127i cell exposed to isotonic Ringer's solution before and after patch excision (at arrow) during application of alternating pulses (0.5-s duration, 10-s interval) from 0 to ±25 mV. Similar results were obtained in 17 experiments. (B) Representative current trace recorded from a macro-patch after excision (at arrowhead in A). The peak current (216 pA at +25 mV) indicates the presence of 21 open channels in this patch. (Inset) the all-point histogram was obtained from 12 different sweeps at +25 mV. Gaussian fits for the first six current peaks yield unitary amplitudes of 12.0, 10.4, 10.9, 12.3, 10.1, and 11.0 pA.

results are similar to what has been found in previous studies (Okada et al., 1994; Okada, 1997).

Excision-induced Activation of Voltage-dependent Large-Conductance Anion Channels

When silent patches from C127i cells bathed in isotonic Ringer's solution were excised, patch conductance rapidly increased up to 2–10 nS (Fig. 4 A). As shown in Fig. 4 B, the patch current inactivated at +25 mV in a stepwise manner revealing unitary events with an amplitude of 10–12 pA.

In excised patches, voltage and time dependency of inactivation of macro-patch currents (Fig. 5 A) was similar to that of swelling-induced phloretin-insensitive whole-cell currents (Fig. 1 B, b). The shape of the instantaneous current-voltage relationship (Fig. 5 B, open circles) was more linear compared with whole-cell currents, but the steady-state current similarly displayed portions with "negative slope resistance" at potentials of greater than or equal to +20 and less than or equal to −30 mV (Fig. 5 B, closed circles). The I-V curve obtained during ramp clamp also displayed similar inactivation (Fig. 5 C). Steady-state P_o values estimated from current responses in macro-patches (containing a number of channels) to step pulses (Fig. 5 A) and ramp pulses (Fig. 5 C) were both plotted against voltages in Fig. 5 D (closed circles and solid line, respectively), together with steady-state P_o estimated from the phloretin-insensitive component of the swelling-activated whole-cell currents (Fig. 1 B, b). The bell-shaped voltage dependency of open-channel probability of the macro-patch current was strikingly similar to that of whole-cell currents (Fig. 5 D, triangles). Based on these observations, we conclude that voltage-dependent large-conductance channels were responsible for the phloretin-insensitive volume-dependent whole-cell current. This conclusion was further confirmed in studies evaluating anion selectivity and pharmacology of this voltage-dependent large-conductance channel (see next paragraph).

Channels activated in inside-out patches had a conductance of 398 ± 9 pS and a linear symmetrical i-V relationship (Fig. 6 A, open circles). Neither the shape of the i-V relationship nor the reversal potential changed when Na^+ in the bath (Fig. 6 A, open squares) or in the pipette (Fig. 6 A, open triangles) solution was replaced with TEA^+. In contrast, replacement of chloride with other anion species in the bathing solution had a profound effect on the single-channel i-V relationship. Also, the reversal potential became more positive for iodide and bromide ions and more negative for fluoride, aspartate, and glutamate (Fig. 6 B). The calculated permeability ratios showed a selectivity sequence of I > Br > Cl > F > phosphate > aspartate ~ glutamate, as summarized in Table I. When NaCl concentration was lowered by replacement with mannitol, shifts in reversal potential yielded P_{Cl}/P_{Na} = 21–26 (Fig. 6 C). Thus, it appears that the large-conductance

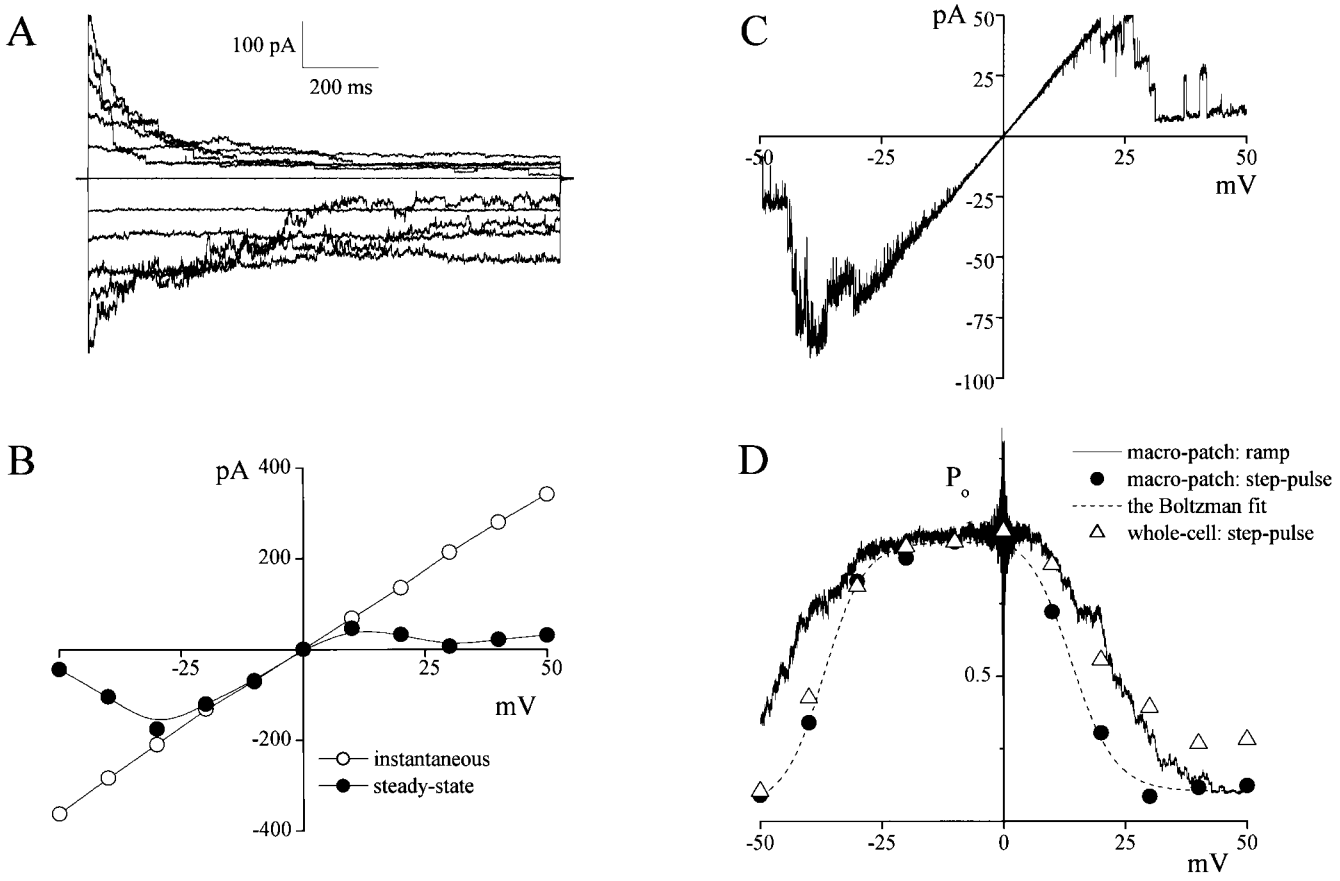

FIGURE 5. Voltage-dependent inactivation of large-conductance single-channel currents recorded in macro-patches. (A) Representative current traces recorded upon application of step pulses (1-s duration) from 0 to ±50 mV in 10-mV increments in a macro-patch (containing 20 active channels) excised from a C127i cell. (B) I-V relationship of instantaneous (open circles) and steady-state (closed circles) currents, from the recording shown in A, measured at the beginning and end of current responses to step pulses. (C) Representative steady-state ramp I-V records from a macro-patch (containing five active channels) excised from a C127i cell. A ramp pulse was applied from +50 to −50 mV at the rate of 10 mV/s. (D) Voltage dependence of steady-state open-channel probability. Closed circles represent the ratio of steady-state macro-patch current to instantaneous macro-patch current (from B). Dashed line is the Boltzmann fit for closed circles with V_0 = +13.9 and −36.9 mV for positive and negative potentials, respectively. The solid line represents the ensemble-averaged current of 11 consecutive current responses to ramp pulses as shown in (C). These P_o values were calculated as $P_o = (I/V)/G_{max}$, where I is the patch current, V is the voltage, and G_{max} is the maximal patch conductance at 0 mV. Open triangles represent the ratio of steady-state whole-cell current to instantaneous whole-cell current (from Fig. 1 B, c).

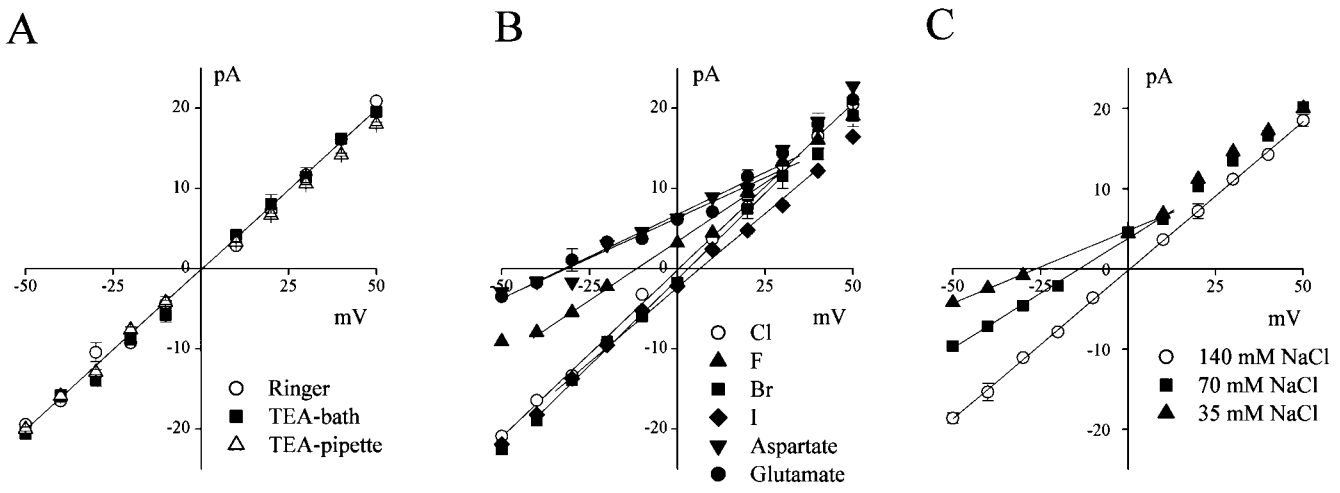

FIGURE 6. Anion selectivity of large-conductance single-channel currents recorded from inside-out patches. Each i-V relationship is corrected for the liquid junction potentials. Each data point represents an average of 3–12 measurements. Open circles represent control data. Solid lines represent linear fits. (A) Effects of substitution of Na^+ in the bath (squares) or pipette solution (triangles) with TEA^+; (B) effects of replacement of bath Cl^- (closed symbols) with other anion species (as indicated); and (C) effects of reduction in bath NaCl concentration by isosmotic replacement with mannitol (closed symbols). The P_{Cl}/P_{Na} values were 26.3 and 21.3 from reversal potentials of 13.9 ± 1.1 and 26.3 ± 1.1 mV at 70 and 35 mM NaCl, respectively. The SEM values are shown by vertical bars where the values exceed the symbol size.

TABLE I

Ionic Selectivity of Large-Conductance Anion Channel

Ion	E_{rev}	P_X/P_{Cl}	*n*
Fluoride	−11.6 ± 1.3	0.61 ± 0.04	5
Chloride	0	1	–
Bromide	3.1 ± 0.5	1.14 ± 0.02	5
Iodide	6.4 ± 0.7	1.31 ± 0.04	5
Aspartate	−31.6 ± 2.1	0.23 ± 0.03	5
Glutamate	−32.2 ± 1.8	0.22 ± 0.02	5
Phosphate	−13.5 ± 2.8	0.43 ± 0.07	6

Reversal potentials were calculated from the fits to the linear part of the I-V curves as shown in Fig. 7 B. P_X/P_{Cl} was calculated by Eq. 3.

channels are not only largely selective to Cl^-, but are also permeable to large organic anions as well.

Open-channel Blocking of the Large-Conductance Channel Current by ATP from Both Outside and Inside

In the outside-out patches, single-channel amplitude of the large-conductance channel was significantly decreased by extracellular ATP (10 mM added to the bath) at positive potentials, whereas there was not much of an effect at negative potentials (Fig. 7, A and B). The effects of different ATP concentrations on single-channel i-V relationships obtained in the outside-out mode are shown in Fig. 7 C. The dose–response curve for the outward current could be well fitted with an equation for a single ATP-binding site (Eq. 1) with a K_d of 12.3 ± 1.1 mM (Fig. 7 D). This site is located at an electrical distance δ of 0.47 ± 0.07 from the external entrance to the pore, as evidenced by the Boltzmann fit (Eq. 2) of the voltage-dependent blockade (Fig. 7 E).

In the inside-out mode, in contrast to the outside-out mode, inward currents at negative potentials were depressed by intracellular ATP (10 mM added to the bath) more significantly than the outward currents (Fig. 8, A and B). Dose-dependent blockade of ATP applied to the intracellular solution is shown in Fig. 8 C. This block was very profound for inward currents and could be well described by binding of ATP to a single binding site with K_d = 12.9 ± 0.6 mM (Fig. 8 D) lo-

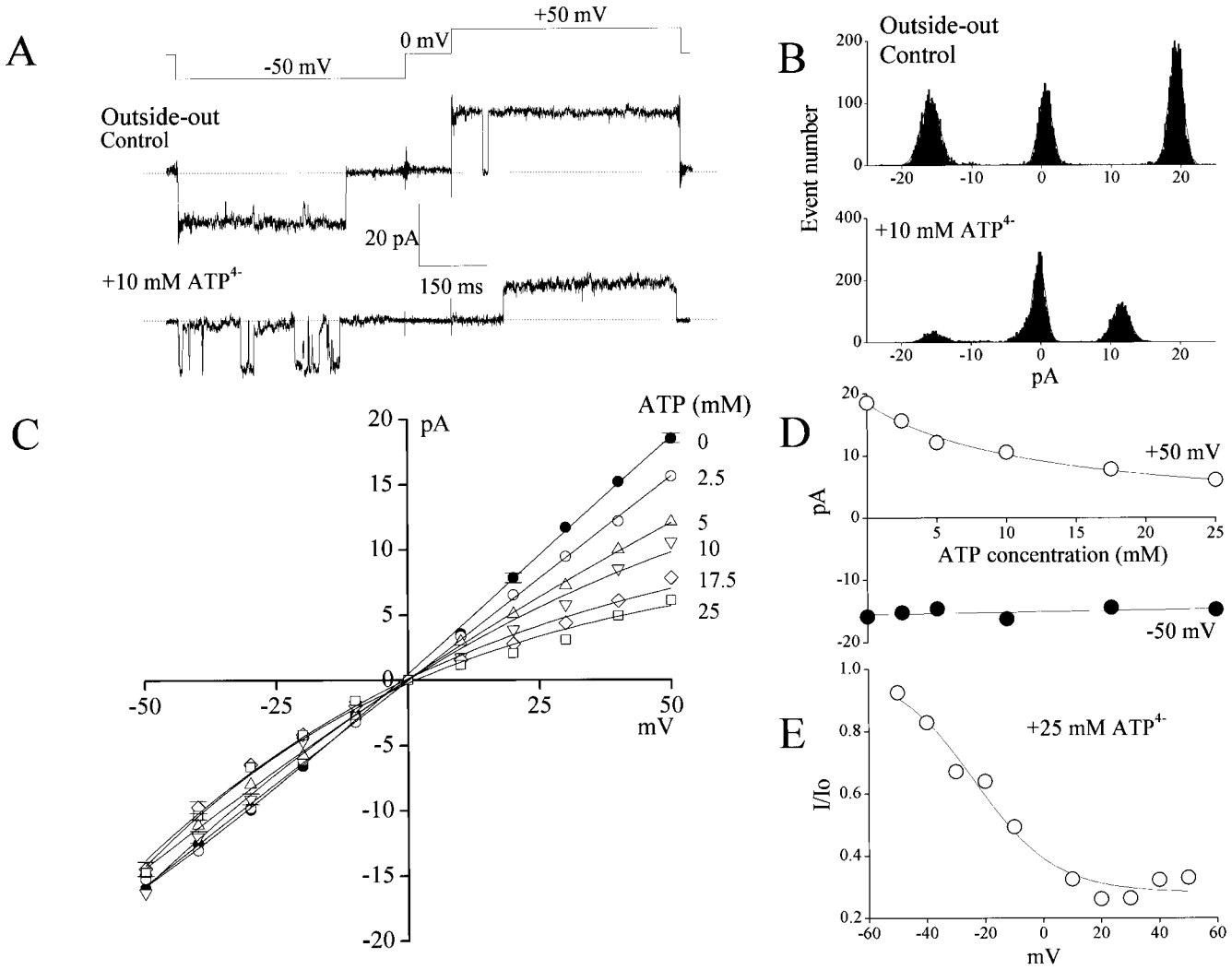

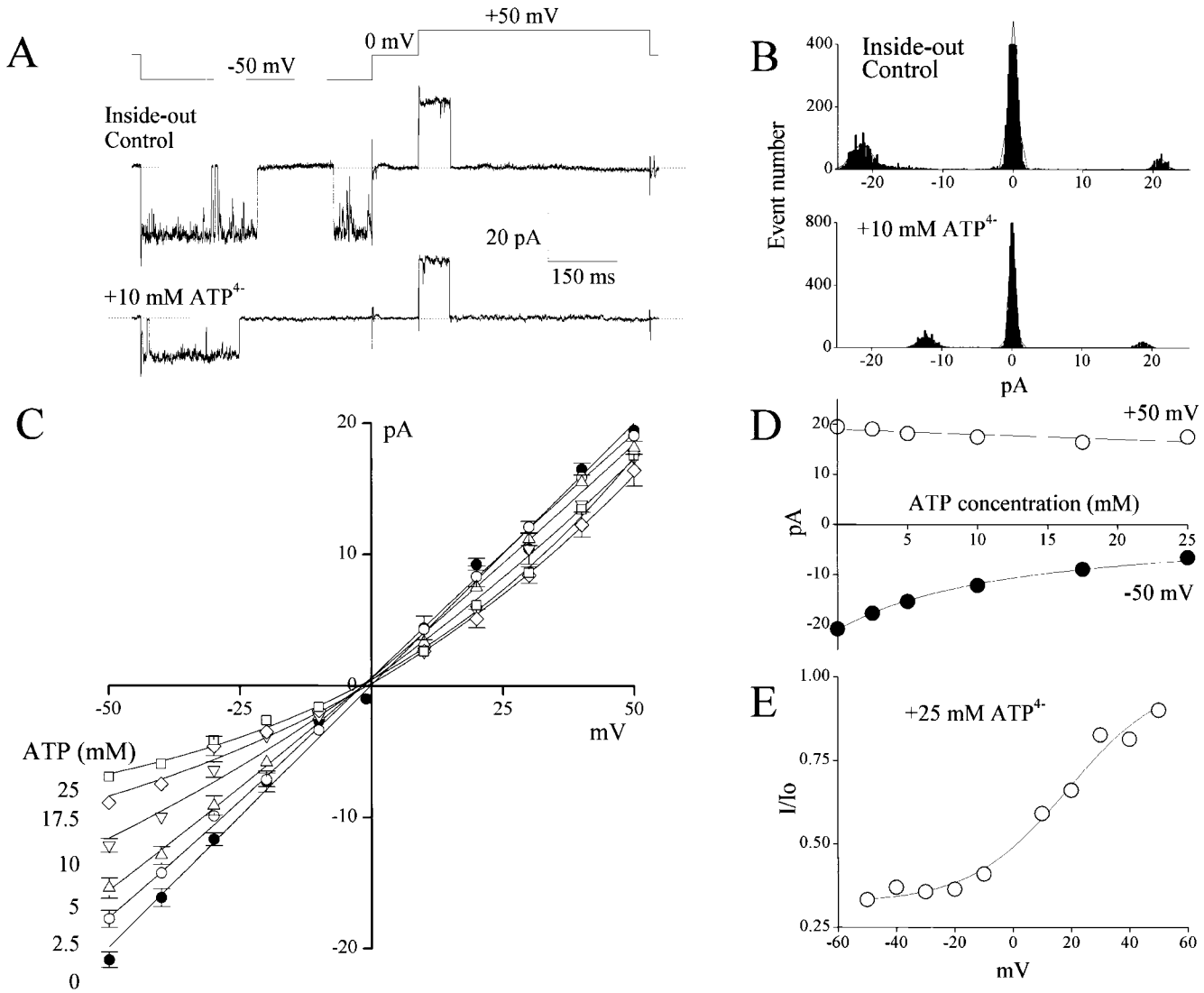

FIGURE 8. Open-channel block of large-conductance anion channel by ATP from the intracellular side. Data were obtained from inside-out patches excised from C127i cells. A and B are the same as those in Fig. 7. C–E are also the same as those in Fig. 8, except that each data point in C and D represents the mean ± SEM of five to seven experiments.

cated at the distance of $\delta = 0.40 \pm 0.06$ from the internal mouth of the pore (Fig. 8 E).

Taken together, we conclude that ATP causes a voltage-dependent open-channel blockade of these large-conductance anion channels. This inhibitory effect of ATP is likely to be very fast since no increase in channel noise could be detected, even when the recordings were performed at 5-kHz bandwidth (unpublished data; $n = 8$). Nearly identical values for the two dissociation constants and the halfway location of the binding site strongly suggest that ATP binds to a site located near the center of pore when it is applied from either the extra-

FIGURE 7. Open-channel block of large-conductance anion channel by ATP from the extracellular side. Data were obtained from outside-out patches excised from C127i cells. (A) Representative current traces recorded in the absence (control) and presence of 10 mM ATP in the bath during application of step pulses (0.5-s duration) from 0 to ±50 mV (protocol is shown at the top of the traces). Dashed lines indicate zero-current level. (B) Amplitude histograms of single-channel currents shown in A. (C) Unitary current-voltage (i-V) relationships of large-conductance anion channel currents in the absence and presence of varying ATP concentrations in the bath. Each data point represents the mean ± SEM of 5–12 experiments. The SEM values are shown by vertical bars where the values exceed the symbol size. (D) Concentration-inhibition curve of ATP versus single-channel currents recorded at +50 mV (open circles) and −50 mV (closed circles). Data were taken from C. All the SEM values were smaller than the symbol size. Solid lines represent fits to Eq. 1. (E) Voltage-dependent block of the channel by 25 mM ATP. I and I_0 represent the channel current amplitude in the presence and absence of 25 mM ATP in the bath, respectively. The solid line represents a fit to Eq. 2.

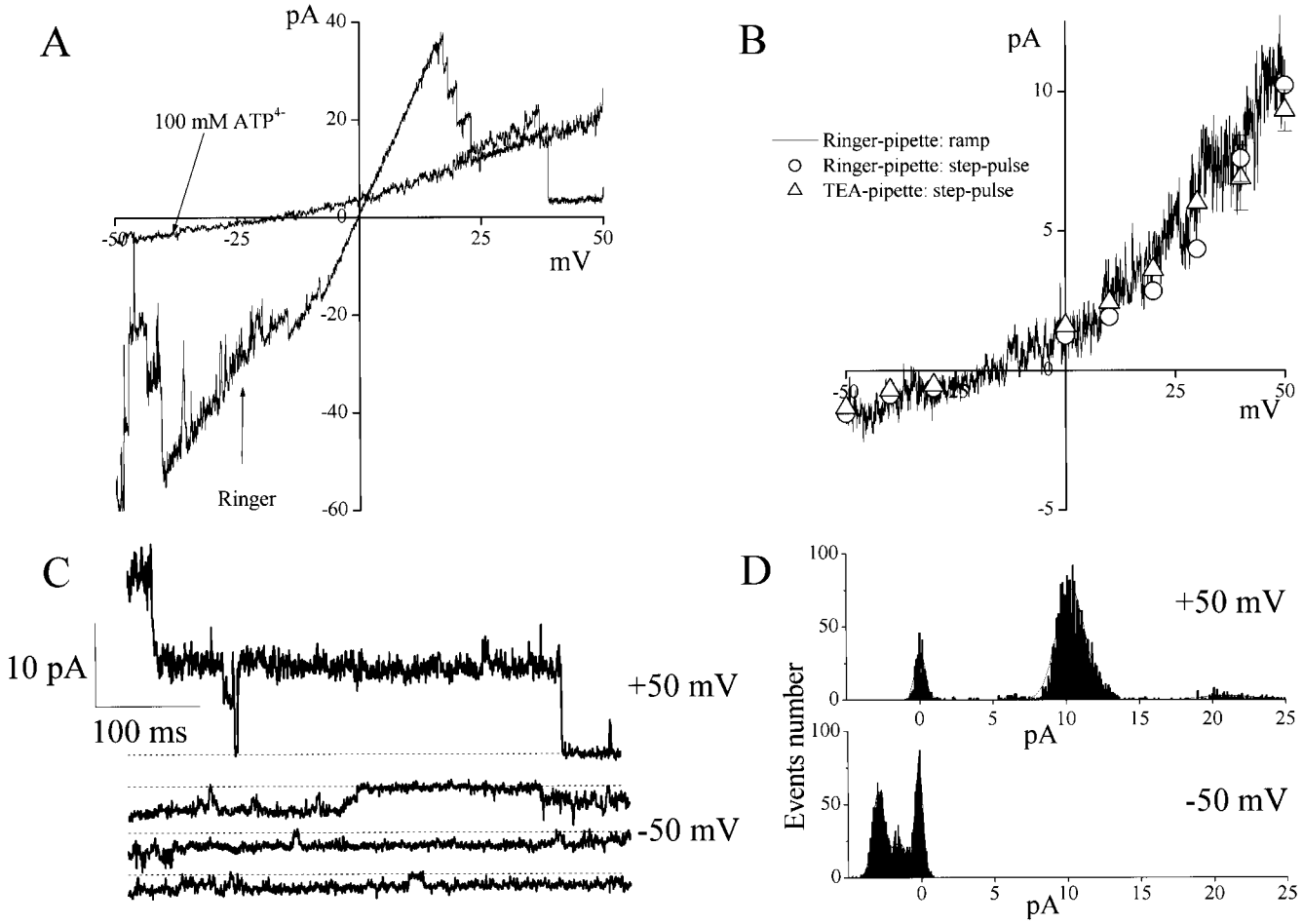

FIGURE 9. ATP permeability of large-conductance anion channel recorded from inside-out patches excised from C127i cells. Currents were recorded in standard Ringer's bath solution or in a 100 mM Na_2ATP bath solution. (A) Representative ramp I-V records from a macro-patch in the absence and presence of 100 mM ATP in the bath. Pipette solution was standard Ringer's. (B) Single-channel i-V relationships in the presence of 100 mM ATP in the bath. Solid line represents ramp i-V, recorded using standard Ringer's as the pipette solution. Open circles and triangles represent the mean ± SEM of 4–21 single-channel currents measured upon application of step pulses at voltages indicated on the abscissa using standard Ringer's and TEA solutions, respectively, as the pipette solution. The SEM values are shown by vertical bars where the values exceed the symbol size. (C) One and three representative traces of single-channel currents recorded at +50 and −50 mV, respectively, in the presence of 100 mM ATP in the bath. The pipette solution was standard Ringer. Dashed lines indicate zero-current level. (D) Amplitude histograms of single-channel currents recorded at ±50 mV. For outward Cl^- currents at +50 mV, peaks correspond to unitary steps of 10.3 ± 1.9 and 10.7 ± 3.2 pA together with a sublevel at ~6.7 pA. For inward ATP^{4-} currents at −50 mV, two peaks corresponding to unitary steps of −1.7 ± 1.1 and −1.4 ± 0.8 pA can be distinguished.

cellular or intracellular side of the membrane patch. Therefore, the large-conductance channel can accommodate ATP anions deep inside the pore lumen.

ATP Permeation through Large-Conductance Anion Channels

When the Ringer's bath solution was replaced with 100 mM ATP^{4-}, current amplitude of an inside-out patch containing a number of large-conductance channels was inhibited, the I-V relationship became outwardly rectifying, and the inactivation gating became less prominent (Fig. 9 A). Small inward currents could be detected both under ramp clamp (Fig. 9, A and B) and by applying step pulses (Fig. 9, B–D). The small inward currents were found to be blocked by 100 μM NPPB or 200 μM SITS, but not Gd^{3+} (30 μM), added to inside-out patches from the intracellular side, whenever the outward currents were blocked (unpublished data; n =

TABLE II

ATP Permeability of Large-Conductance Anion Channel in the Presence of Different Cations in the Pipette Solution

Pipette solution	E_{rev}	P_{ATP}/P_{Cl}	n
Ringer	−16.2 ± 1.9	0.096 ± 0.014	5
Cs-Ringer	−18.2 ± 1.0	0.085 ± 0.006	6
TEA-Ringer	−18.7 ± 1.5	0.083 ± 0.009	5

Reversal potentials obtained from ramp I-V curves after correction for the background currents. The mean values are not significantly different based on t test at P . 0.05. PATP/PCl was calculated using Eq. 5.

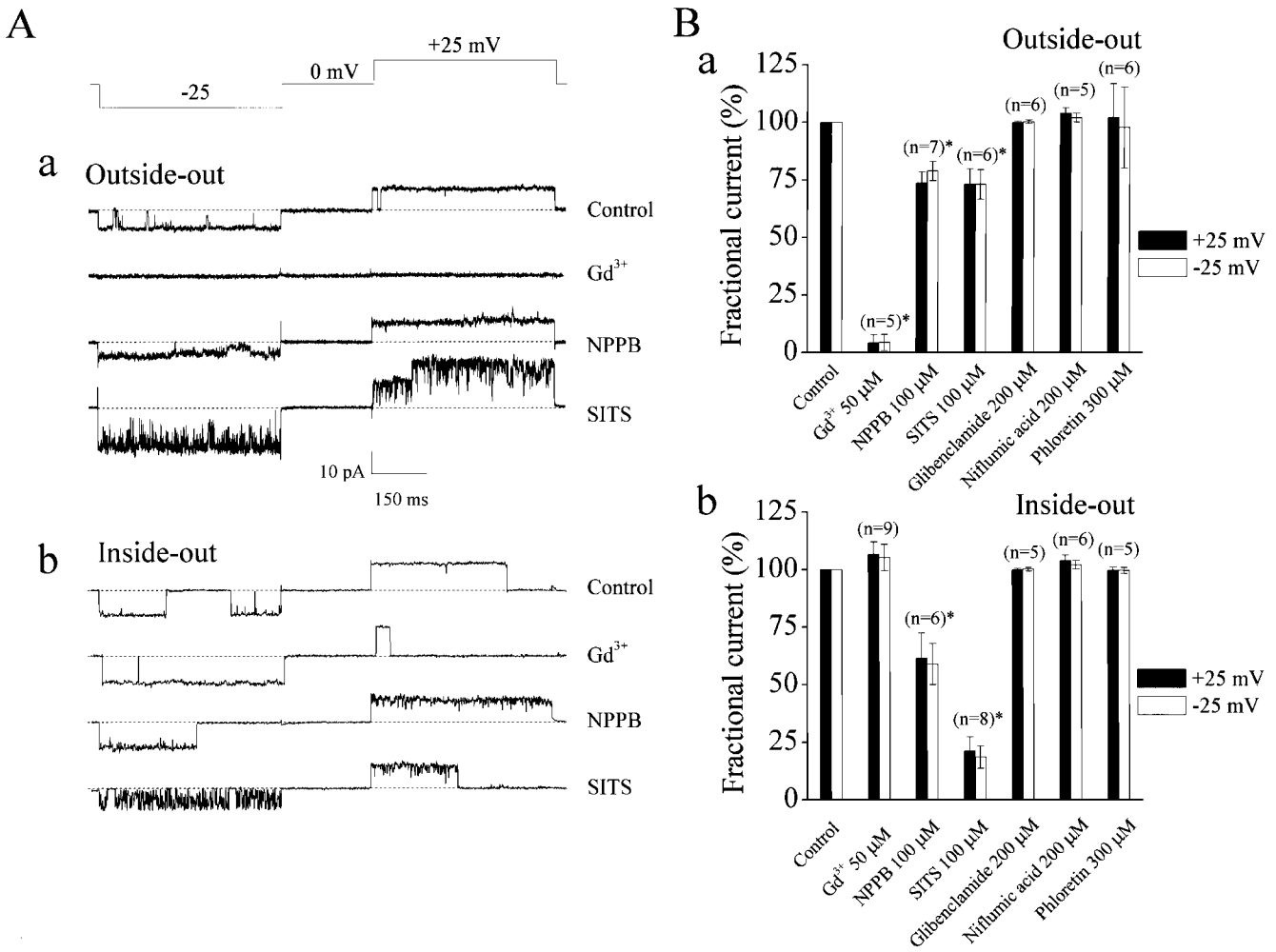

FIGURE 10. Effects of Gd^{3+} and conventional anion channel blockers on large-conductance anion single-channel currents in outside-out and inside-out patches excised from C127i cells. (A) Representative current traces recorded from outside-out (a) and inside-out (b) patches in the absence (control) or presence of 30 μM Gd^{3+}, 100 μM NPPB, or 100 μM SITS during application of step pulses (protocol is shown at the top of the traces). Dashed lines indicate zero-current level. (B) Effects of Gd^{3+} and conventional anion channel blockers on mean macro-patch currents recorded at ±25 mV from outside-out (a) and inside-out (b) patches. Data were normalized to the mean current measured before application of drugs after correction for the background current. Each column represents the mean ± SEM (vertical bar). $*P < 0.02$ vs. control.

3 each). If the inward current was due to sodium flux from the pipette, then the reversal potential of −20 mV would suggest $P_{Cl}/P_{Na} = 2.2$, which is ∼10 times less than it was actually measured to be in our experiments (see data in Fig. 6 C). When Na^+ in the pipette was replaced with Cs^+ or TEA^+ in the presence of 100 mM ATP^{4-} in the bath, the i-V relationship and the reversal potential were not affected (Fig. 9 B and Table II). Therefore, it is unlikely that the inward current is due to cationic flux from the pipette. Since no other anion except ATP^{4-} was present in the bath, the inward current component should be due to the conductance to ATP^{4-}. However, it is also possible that this inward current could be carried by inorganic phosphates produced by ATP degradation, since the channel exhibited a considerable permeability to phosphate (Table I). To produce a reversal potential of −20 mV, ∼40 mM of HPO_4^{2-} would be needed in the absence of significant ATP^{4-} permeability of this channel. However, luciferin-luciferase measurements of the 100-mM ATP solutions, used in these experiments, gave an ATP concentration of 103 ± 3 mM ($n = 5$), which is not statistically different from 100 mM, suggesting that no significant ATP degradation occurred in the solutions used in our experiments. There is a possibility that the effects of 100 mM ATP were simply due to divalent ion chelation by ATP. However, single-channel conductance and channel gating were not essentially affected by applying Mg^{2+}- and Ca^{2+}-free Ringer's solution containing 1 mM EDTA (unpublished data; $n = 9$). Thus, it is concluded that the large-conductance anion channel is ATP-permeable with a P_{ATP}/P_{Cl} ratio of 0.08–0.1 (Table II). This

value is comparable to the permeability of the ATP-conductive pathway in CFTR-expressing cells (P_{ATP}/P_{Cl} = 0.2 [Reisin et al., 1994], 0.3 [Sugita et al., 1998], and 0.1–0.2 [Cantiello et al., 1998]).

Pharmacological Profile of Large-Conductance Single-channel Activity

Fig. 10 illustrates a pharmacological profile of the large-conductance anion channel at the single-channel level. This channel in outside-out patches was readily blocked by bath application of 30 μM Gd^{3+} (Fig. 10, A and B, a, respectively), whereas, in the inside-out mode, 30–500 μM Gd^{3+} had no effect on the channel activity from the intracellular side (Fig. 10, A and 10 B, b, respectively). NPPB, produced a fast open-channel block: in the presence of 100 μM NPPB in the bathing solution, the large-conductance channels recorded in outside-out (a) and inside-out (b) patches had smaller amplitudes with increased noise (Fig. 10 A). Another conventional Cl^- channel blocker, SITS, produced a profound flickery open-channel block that is shown in traces from both outside-out (Fig. 10 A, a) and inside-out (Fig. 10 A, b) patches. The large-conductance anion single-channel in C127i cells was insensitive to 200 μM niflumic acid, 200 μM glibenclamide, and 300 μM phloretin from both extracellular (Fig. 10 B, a) and intracellular (Fig. 10 B, b) sides. Thus, the pharmacological properties of the single-channel currents from the voltage-dependent, large-conductance anion channel are virtually identical to those of the phloretin-insensitive volume-dependent whole-cell currents (Figs. 1 B and 2 B).

Pharmacological Profile of Swelling-induced ATP Release

Fig. 11 A summarizes the pharmacological profiles of the swelling-induced ATP release from C127i cells under standard experimental conditions (37°C and 56% hypotonic stress) used in our previous paper (Hazama et al., 2000b). The application of extracellular 30 μM Gd^{3+} nearly completely inhibited swelling-induced ATP release from C127i cells, as was previously observed in C127/CFTR cells (Hazama et al., 2000b). SITS and NPPB also effectively suppressed the release of ATP from swollen C127i cells, whereas phloretin, glibenclamide, and niflumic acid had no significant effect on the release of ATP. Quantitative differences of the effects of SITS and NPPB from those observed in patch-clamp experiments might be due to differences in experimental conditions: higher incubation temperature and stronger hypotonic stimulation for ATP release measurements.

We then measured ATP release from C127i cells under the conditions similar to those for patch-clamp experiments (at 25°C and 71% osmolality). Fig. 11 B summarizes the pharmacological profiles of the swelling-induced ATP release observed under these conditions. Extracellular Gd^{3+} again exhibited a strong inhibiting effect on the ATP release, whereas extracellular SITS and NPPB were less effective, and phloretin, glibenclamide, and niflumic acid had again no significant effect on the release of ATP. The pharmacological profile of swelling-induced ATP release is essentially the same as those found for whole-cell (Figs. 1 B and 2 B) and single-channel currents (Fig. 10).

DISCUSSION

In response to many different stimuli, ATP has been demonstrated to be released from neuronal and non-neuronal cells. One reason that ATP may be released into extracellular fluid is to serve as a signaling molecule involved in cell–cell communication in a wide variety of cell types (Dubyak and El-Moatassim, 1993; Ralevic and Burnstock, 1998; Fields and Stevens, 2000) including mammary epithelial cells and myofibroblasts (Enomoto et al., 1994; Nakano et al., 1997). Among the stimuli for noncytolytic release of ATP, the most effective one is mechanical stress (Osipchuk and Cahalan, 1992; Enomoto et al., 1994; Grygorczyk and Hanrahan, 1997; Sprague et al., 1998; Watt et al., 1998; Pedersen et al., 1999; Homolya et al., 2000; Sauer et al., 2000) or osmotic swelling (Wang et al., 1996; Roman et al., 1997, 1999; Feranchak et al., 1998; Hazama et al., 1998b, 1999, 2000a,b; Mitchell et al., 1998; Taylor et al., 1998; Light et al., 1999; Musante et al., 1999). Although it is clear that exocytotic ATP release from secretory granules occurs in some cell types including mast cells (Osipchuk and Cahalan, 1992), neurons (Silinsky, 1975; Zimmermann, 1994; Jo and Schlichter, 1999), and pancreatic β cells (Hazama et al., 1998a), the mechanism by which ATP is moved across the plasma membrane is not known in other cell types.

Since most ATP molecules exist in anionic forms at physiological pH, there is a possibility that some anion channels can conduct ATP. In fact, recent patch-clamp studies have provided data showing ATP-conducting currents in association with the expression of CFTR (Reisin et al., 1994; Schwiebert et al., 1995; Cantiello et al., 1997, 1998; Pasyk and Foskett, 1997; Lader et al., 2000) or that of MDR1 (Abraham et al., 1993; Bosch et al., 1996; Roman et al., 1999), and ATP currents independent of CFTR or MDR1 expression (Sugita et al., 1998; Bodas et al., 2000).

Previously, in mouse mammary C127i cells, swelling-induced ATP release was shown to be independent of CFTR and VSOR Cl^- channels (Hazama et al., 2000a,b). We have recently found an ATP-conductive maxi anion channel at the basolateral membrane of rabbit renal macula densa cells, where it may function to release ATP as a signal for tubuloglomerular feedback (Bell et al., 2000). Thus, we examined the possibility that maxi anion channels might also be involved in ATP release from swollen C127i cells.

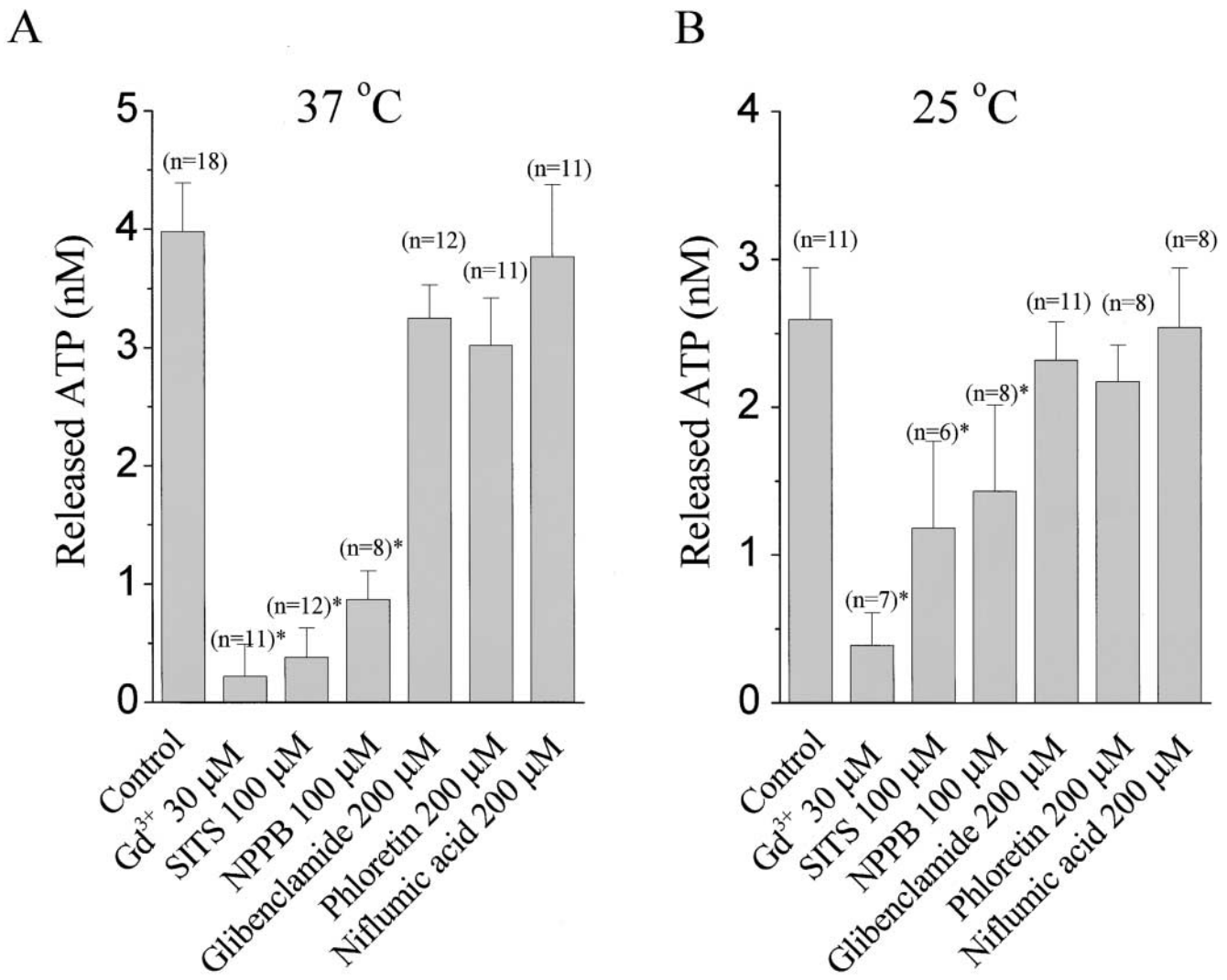

FIGURE 11. Effects of Gd^{3+} and conventional anion channel blockers on swelling-induced ATP release from C127i cells at 37°C and 56% osmolality (A) and at 25°C and 71% osmolality (B). Each column represents the mean ± SEM (bars). The data are corrected for the background ATP release under isotonic conditions. *Significantly different from the control at $P < 0.05$.

Here, we identified and characterized the volume-dependent VDACL anion channels in C127i cells. We conclude that this channel serves as a pathway for swelling-induced ATP release in this cell line for the following reasons: (1) this channel is activated by osmotic cell swelling in both cell-attached and whole-cell modes; (2) the channel pore has an ATP-binding site that is about halfway from both extracellular and intracellular sides, thereby resulting in ATP accumulation within the pore; (3) the current that was carried by ATP^{4-} was actually detected in inside-out patches; (4) this channel shares the same pharmacological profile as swelling-induced ATP release, i.e., sensitivity to Gd^{3+}, SITS, and NPPB as well as insensitivity to phloretin, niflumic acid, and glibenclamide; and (5) swelling-induced activation of this channel was facilitated in CFTR-expressing cells in agreement with the upregulation of swelling-induced ATP release by CFTR (Hazama et al., 1998b, 2000b). Assuming that intracellular ATP and Cl^- concentrations are 2.5 and 25 mM, respectively, it can be estimated that VDACL anion channels may transport $\sim 10^5$ ATP^{4-} s^{-1} at −30 mV. This is comparable to the measured rate of ATP release, which was 2×10^4 s^{-1} $cell^{-1}$ in response to cell swelling (Hazama et al., 2000b).

Biophysical and physiological characteristics of VDACL anion channels in C127i cells are quite different, in a number of ways, compared with VSOR Cl^- channels in C127/CFTR cells (Hazama et al., 2000b) and other cell types (Strange et al., 1996; Nilius et al., 1997; Okada, 1997), although both channels are activated by osmotic cell swelling. First, single-channel conductance of the VDACL channel (~400 pS) was much greater than that of VSOR channels (50–70 pS). Second, single-channel current-voltage relationship was linear

for VDACL channels, but was outwardly rectifying for VSOR channels. Third, voltage-dependent inactivation was observed in VDACL currents not only at large positive potentials, but also at large negative potentials, thus exhibiting the bell-shaped voltage dependency of open-channel probability, whereas it was observed in VSOR currents only at large positive potentials. Fourth, VDACL, but not VSOR, channels were activated in cell-attached patches when cells were exposed to a hypotonic solution after giga-sealed formation. Fifth, VDACL, but not VSOR, channels could be activated by patch excision without reducing bath osmolarity. Sixth, the presence of intracellular ATP was not required for VDACL channel activity, but was a prerequisite to VSOR channel activity. The pharmacological profile for inhibition of VDACL channel activity was also distinct from that of VSOR channel. VDACL channels were sensitive to Gd^{3+}, which was ineffective for VSOR channels, and insensitive to known blockers of VSOR channels, such as phloretin, niflumic acid, and glibenclamide.

The large unitary conductance and bell-shaped voltage dependency of VDACL channels in C127i cells are similar to those of the voltage-dependent anion channel (VDAC) expressed in the outer mitochondrial membrane (Schein et al., 1976; Colombini, 1979; Wunder and Colombini, 1991). Such VDAC-like (VDACL) anion channels have been observed in a wide variety of cell types (Strange et al., 1996), suggesting some general physiological role of this channel. VDACL channels in C127i cells also resemble mitochondrial VDAC with respect to the open-channel block by ATP (Rostovtseva and Bezrukov, 1998) and ATP permeability or conductivity (Rostovtseva and Colombini, 1997; Rostovtseva and Bezrukov, 1998). Also, a growing body of evidence has been accumulating for the expression of VDAC isoforms in the plasma membrane (Thinnes et al., 1989; Dermietzel et al., 1994; Jakob et al., 1995; Eben-Brunnen et al., 1998; Bàthori et al., 1999; Buettner et al., 2000; Steinacker et al., 2000). Maxi anion channels have been suggested to be formed by plasmalemmal VDAC in rat astrocytes (Dermietzel et al., 1994) and PC12 cells (Buettner et al., 2000). Taken together, it is possible that a plasmalemmal isoform of VDAC is responsible for the VDACL anion channel in C127i cells, although direct verification remains for future studies.

Previous studies have suggested various signaling pathways involved in activation of the VDACL anion channels in other cell types: G proteins (Schwiebert et al., 1990, 1992; Sun et al., 1992, 1993; McGill et al., 1993; Mitchell et al., 1997), Ca^{2+} (Light et al., 1990; Kawahara and Takuwa, 1991; Groschner and Kukovetz, 1992), PKC (Groschner and Kukovetz, 1992; Schwiebert et al., 1992), actin (Schwiebert et al., 1994), NK-1 receptor (Sun et al., 1992, 1993), adenosine A1 receptor (Schwiebert et al., 1992), and estrogen receptor (Hardy and Valverde, 1994; Li et al., 2000). The exact activation mechanism of the VDACL anion channel in mammary C127i cells is under current investigation. The mechanism of facilitating the effect of CFTR expression on swelling-induced activation also remains to be studied.

The authors are grateful to P.D. Bell for reading the manuscript, to S. Tanaka and K. Shigemoto for technical assistance, and to T. Okayasu for secretarial assistance.

This work was supported by Grant-in-Aid for Scientific Research (to R.Z. Sabirov) and by that for Priority Areas of "ABC Proteins" (to Y. Okada) from the Ministry of Education, Culture, Sports, Science and Technology of Japan, and by grants from Houansha Foundation and Salt Science Foundation (to Y. Okada).

Submitted: 2 March 2001
Revised: 16 July 2001
Accepted: 18 July 2001

REFERENCES

Abraham, E.H., A.G. Prat, L. Gerweck, T. Seneveratne, R.J. Arceci, R. Kramer, G. Guidotti, and H.F. Cantiello. 1993. The multidrug resistance (*mdr1*) gene product functions as an ATP channel. *Proc. Natl. Acad. Sci. USA.* 90:312–316.

Bàthori, G., I. Parolini, F. Tombola, I. Szabò, A. Messina, M. Olive, V. De Pinto, M. Lisanti, M. Sargiacomo, and M. Zoratti. 1999. Porin is present in the plasma membrane where it is concentrated in caveolae and caveolae-related domains. *J. Biol. Chem.* 274:29607–29612.

Bell, P.D., J.-Y. Lapointe, R. Sabirov, S. Hayashi, and Y. Okada. 2000. Maxi-chloride channel in macula densa cells: possible pathway for ATP release. *FASEB J.* 14:A134. (Abstr.)

Bodas, E., J. Aleu, G. Pujol, M. Martin-Satue, J. Marsal, and C. Solsona. 2000. ATP crossing the cell plasma membrane generates an ionic current in *Xenopus* oocytes. *J. Biol. Chem.* 275:20268–20273.

Bosch, I., G.R. Jackson, Jr., J.M. Croop, and H.F. Cantiello. 1996. Expression of *Drosophila melanogaster* P-glycoproteins is associated with ATP channel activity. *Am. J. Physiol.* 271:C1527–C1538.

Buettner, R., G. Papoutsoglou, E. Scemes, D.C. Spray, and R. Dermietzel. 2000. Evidence for secretory pathway localization of a voltage-dependent anion channel isoform. *Proc. Natl. Acad. Sci. USA.* 97:3201–3206.

Cantiello, H.F., G.R. Jackson, Jr., A.G. Prat, J.L. Gazley, J.N. Forrest, Jr., and D.A. Ausiello. 1997. cAMP activates an ATP-conductive pathway in cultured shark rectal gland cells. *Am. J. Physiol.* 272: C466–C475.

Cantiello, H.F., G.R. Jackson, Jr., C.F. Grosman, A.G. Prat, S.C. Borkan, Y. Wang, I.L. Reisin, C.R. O'Riordan, and F.A. Ausiello. 1998. Electrodiffusional ATP movement through the cystic fibrosis transmembrane conductance regulator. *Am. J. Physiol.* 274: C799–C809.

Colombini, M. 1979. A candidate for the permeability pathway of the outer mitochondrial membrane. *Nature.* 279:643–645.

Dermietzel, R., T.-K. Hwang, R. Buettner, A. Hofer, E. Dotzler, M. Kremer, R. Deutzmann, F.P. Thinnes, G.I. Fishman, D.C. Spray, and D. Siemen. 1994. Cloning and in situ localization of a brain-derived porin that constitutes a large-conductance anion channel in astrocytic plasma membranes. *Proc. Natl. Acad. Sci. USA.* 91: 499–503.

Dubyak, G.R., and C. El-Moatassim. 1993. Signal transduction via P_2-purinergic receptors for extracellular ATP and other nucleotides. *Am. J. Physiol.* 265:C577–C606.

Eben-Brunnen, J., S. Reymann, L.A. Awni, T. Cole, T. Hellmann, K.P.

Hellmann, G. Paetzold, J. Kleineke, F.P. Thinnes, H. Götz, and N. Hilschmann. 1998. Lentil lectin enriched microsomes from the plasma membrane of the human B-lymphocyte cell line H2LCL carry a heavy load of type-1 porin. *Biol. Chem.* 379:1419–1426.

Enomoto, K., K. Furuya, S. Yamagishi, T. Oka, and T. Maeno. 1994. The increase in the intracellular Ca^{2+} concentration induced by mechanical stimulation is propagated via release of pyrophosphorylated nucleotides in mammary epithelial cells. *Pflügers Arch.* 427:533–542.

Fan, H.T., S. Morishima, H. Kida, and Y. Okada. 2001. Phloretin differentially inhibits volume-sensitive and cyclic AMP-activated, but not Ca-activated, Cl^- channels. *Br. J. Pharmacol.* In press.

Feranchak, A.P., R.M. Roman, E.M. Schwiebert, and J.G. Fitz. 1998. Phosphatidylinositol 3-kinase contributes to cell volume regulation through effects on ATP release. *J. Biol. Chem.* 273:14906–14911.

Fields, R.D., and B. Stevens. 2000. ATP: an extracellular signaling molecule between neurons and glia. *Trends Neurosci.* 23:625–633.

Groschner, K., and W.R. Kukovetz. 1992. Voltage-sensitive chloride channels of large conductance in the membrane of pig aortic endothelial cells. *Pflügers Arch.* 421:209–217.

Grygorczyk, R., and J.W. Hanrahan. 1997. CFTR-independent ATP release from epithelial cells triggered by mechanical stimuli. *Am. J. Physiol.* 272:C1058–C1066.

Grygorczyk, R., J.A. Tabcharani, and J.W. Hanrahan. 1996. CFTR channels expressed in CHO cells do not have detectable ATP conductance. *J. Membr. Biol.* 151:139–148.

Hardy, S.P., and M.A. Valverde. 1994. Novel plasma membrane action of estrogen and antiestrogens revealed by their regulation of a large conductance chloride channel. *FASEB J.* 8:760–765.

Harned, H., and B.B. Owen. 1958. The Physical Chemistry of Electrolytic Solutions. Reinhold, New York. 803 pp.

Hazama, A., S. Hayashi, and Y. Okada. 1998a. Cell surface measurements of ATP release from single pancreatic beta cells using a novel biosensor technique. *Pflügers Arch.* 437:31–35.

Hazama, A., A. Miwa, T. Miyoshi, T. Shimizu, and Y. Okada. 1998b. ATP release from swollen or CFTR-expressing epithelial cells. *In* Cell Volume Regulation: The Molecular Mechanism and Volume Sensing Machinery. Y. Okada, editor. Elsevier, Amsterdam. 93–98.

Hazama, A., T. Shimizu, Y. Ando-Akatsuka, S. Hayashi, S. Tanaka, E. Maeno, and Y. Okada. 1999. Swelling-induced, CFTR-independent ATP release from a human epithelial cell line: lack of correlation with volume-sensitive Cl^- channels. *J. Gen. Physiol.* 114:525–533.

Hazama, A., Y. Ando-Akatsuka, H.-T. Fan, S. Tanaka, and Y. Okada. 2000a. CFTR-dependent and -independent ATP release induced by osmotic swelling. *In* Control and Disease of Sodium Dependent Transportation Proteins and Ion Channels. Y. Suketa, E. Carafoli, M. Lazduvski, K. Mikoshiba, Y. Okada and E.M. Wright, editors. Elsevier, Amsterdam. 429–431.

Hazama, A., H.T. Fan, I. Abdullaev, E. Maeno, S. Tanaka, Y. Ando-Akatsuka, and Y. Okada. 2000b. Swelling-activated, cystic fibrosis transmembrane conductance regulator-augmented ATP release and Cl^- conductances in murine C127 cells. *J. Physiol.* 523:1–11.

Homolya, L., T.H. Steinberg, and R.C. Boucher. 2000. Cell to cell communication in response to mechanical stress via bilateral release of ATP and UTP in polarized epithelia. *J. Cell Biol.* 150: 1349–1359.

Jakob, C., H. Götz, T. Hellmann, K.P. Hellmann, S. Reymann, H. Flörke, F.P. Thinnes, and N. Hilschmann. 1995. Studies on human porin: XIII. The Type-1 VDAC 'Porin 31HL' biotinylated at the plasmalemma of trypan blue excluding human B lymphocytes. *FEBS Lett.* 368:5–9.

Jiang, Q., D. Mak, S. Devidas, E.M. Schwiebert, A. Bragin, Y. Zhang, W.R. Skach, W.B. Guggino, J.K. Foskett, and J.F. Engelhardt. 1998. Cystic fibrosis transmembrane conductance regulator-associated ATP release is controlled by a chloride sensor. *J. Cell Biol.* 143:645–657.

Jo, Y.-H., and R. Schlichter. 1999. Synaptic corelease of ATP and GABA in cultured spinal neurons. *Nat. Neurosci.* 2:241–245.

Kawahara, K., and N. Takuwa. 1991. Bombesin activates large-conductance chloride channels in Swiss 3T3 fibroblasts. *Biochem. Biophys. Res. Commun.* 177:292–298.

Lader, A.S., Y.F. Xiao, C.R. O'Riordan, A.G. Prat, G.R. Jackson, Jr., and H.F. Cantiello. 2000. cAMP activates an ATP-permeable pathway in neonatal rat cardiac myocytes. *Am. J. Physiol.* 279:C173–C187.

Li, C., M. Ramjeesingh, and C.E. Bear. 1996. Purified cystic fibrosis transmembrane conductance regulator (CFTR) does not function as an ATP channel. *J. Biol. Chem.* 271:11623–11626.

Li, Z., Y. Niwa, S. Sakamoto, X. Chen, and Y. Nakaya. 2000. Estrogen modulates a large conductance chloride channel in cultured porcine aortic endothelial cells. *J. Cardiovasc. Pharmacol.* 35:506–510.

Light, D.B., E.M. Schwiebert, G. Fejes-Toth, A. Naray-Fejes-Toth, K.H. Karlson, F.V. McCann, and B.A. Stanton. 1990. Chloride channels in the apical membrane of cortical collecting duct cells. *Am. J. Physiol.* 258:F273–F280.

Light, D.B., T.L. Capes, R.T. Gronau, and M.R. Adler. 1999. Extracellular ATP stimulates volume decrease in *Necturus* red blood cells. *Am. J. Physiol.* 277:C480–C491.

McGill, J.M., T.W. Gettys, S. Basavappa, and J.G. Fitz. 1993. GTP-binding proteins regulate high conductance anion channels in rat bile duct epithelial cells. *J. Membr. Biol.* 133:253–261.

Mitchell, C.H., L. Wang, and T.J.C. Jacob. 1997. A large-conductance chloride channel in pigmented ciliary epithelial cells activated by GTPγS. *J. Membr. Biol.* 158:167–175.

Mitchell, C.H., D.A. Carre, A.M. Mcglinn, R.A. Stone, and M.M. Civan. 1998. A release mechanism for stored ATP in ocular ciliary epithelial cells. *Proc. Natl. Acad. Sci. USA.* 95:7174–7178.

Musante, L., O. Zagarra-Moran, P.G. Montaldo, M. Ponzoni, and L.J.V. Galietta. 1999. Autocrine regulation of volume-sensitive anion channels in airway epithelial cells by adenosine. *J. Biol. Chem.* 274:11701–11707.

Nakano, H., K. Furuya, S. Furuya, and S. Yamagishi. 1997. Involvement of P_2-purinergic receptors in intracellular Ca^{2+} responses and the contraction of mammary myoepithelial cells. *Pflügers Arch.* 435:1–8.

Nilius, B., J. Eggermont, T. Voets, G. Buyse, V. Manolopoulos, and G. Droogmans. 1997. Properties of volume-regulated anion channels in mammalian cells. *Prog. Biophys. Mol. Biol.* 68:69–119.

Okada, Y. 1997. Volume expansion-sensing outward-rectifier Cl^- channel: fresh start to the molecular identity and volume sensor. *Am. J. Physiol.* 273:C755–C789.

Okada, Y., C.C.H. Petersen, M. Kubo, S. Morishima, and M. Tominaga. 1994. Osmotic swelling activates intermediated-conductance Cl^- channels in human intestinal epithelial cells. *Jpn. J. Physiol.* 44:403–409.

Osipchuk, Y., and M. Cahalan. 1992. Cell-to-cell spread of calcium signals mediated by ATP receptors in mast cells. *Nature.* 359:241–244.

Pasyk, E.A., and J.K. Foskett. 1997. Cystic fibrosis transmembrane conductance regulator-associated ATP and adenosine 3′-phosphate 5′-phosphosulfate channels in endoplasmic reticulum and plasma membranes. *J. Biol. Chem.* 272:7746–7751.

Pedersen, S., S.F. Pedersen, B. Nilius, I.H. Lambert, and E.K. Hoffmann. 1999. Mechanical stress induces release of ATP from Ehrlich ascites tumor cells. *Biochim. Biophys. Acta.* 1416:271–284.

Prat, A.G., I.L. Reisin, D.A. Ausiello, and H.F. Cantiello. 1996. Cellular ATP release by the cystic fibrosis transmembrane conductance regulator. *Am. J. Physiol.* 270:C538–C545.

Ralevic, V., and G. Burnstock. 1998. Receptors for purines and pyri-

midines. *Pharmacol. Rev.* 50:413–492.

Reddy, M.M., P.M. Quinton, C. Haws, J.J. Wine, R. Grygorczyk, J.A. Tabcharani, J.W. Hanrahan, K.L. Gunderson, and R.R. Kopito. 1996. Failure of the cystic fibrosis transmembrane conductance regulator to conduct ATP. *Science.* 271:1876–1879.

Reisin, I.L., A.G. Prat, E.H. Abraham, J.F. Amara, R.J. Grygory, D.A. Ausiello, and H.F. Cantiello. 1994. The cystic fibrosis transmembrane conductance regulator is a dual ATP and chloride channel. *J. Biol. Chem.* 269:20584–20591.

Roman, R.M., A.P. Feranchak, A.K. Davison, E.M. Schwiebert, and J.G. Fitz. 1999. Evidence for Gd^{3+} inhibition of membrane ATP permeability and purinergic signaling. *Am. J. Physiol.* 277:G1222–G1230.

Roman, R.M., Y. Wang, S.D. Lidofsky, A.P. Feranchak, N. Lomri, B.F. Scharschmidt, and J.G. Fitz. 1997. Hepatocellular ATP-binding cassette protein expression enhances ATP release and autocrine regulation of cell volume. *J. Biol. Chem.* 272:21970–21976.

Rostovtseva, T., and M. Colombini. 1997. VDAC channels mediate and gate the flow of ATP: implications for the regulation of mitochondrial function. *Biophys. J.* 72:1954–1962.

Rostovtseva, T.K., and S.M. Bezrukov. 1998. ATP transport through a single mitochondrial channel, VDAC, studied by current fluctuation analysis. *Biophys. J.* 74:2365–2373.

Sauer, H., J. Hescheler, and M. Wartenberg. 2000. Mechanical strain-induced Ca^{2+} waves are propagated via ATP release and purinergic receptor activation. *Am. J. Physiol.* 279:C295–C307.

Schein, S.J., M. Colombini, and A. Finkelstein. 1976. Reconstitution in planar lipid bilayers of a voltage-dependent anion-selective channels obtained from Paramecium mitochondria. *J. Membr. Biol.* 30:99–120.

Schwiebert, E.M., D.B. Light, G. Fejes-Toth, A. Naray-Fejes-Toth, and B.A. Stanton. 1990. A GTP-binding protein activates chloride channels in a renal epithelium. *J. Biol. Chem.* 265:7725–7728.

Schwiebert, E.M., K.H. Karlson, P.A. Friedman, P. Dietl, W.S. Spielman, and B.A. Stanton. 1992. Adenosine regulates a chloride channel via protein kinase C and a G protein in a rabbit cortical collecting duct cell line. *J. Clin. Invest.* 89:834–841.

Schwiebert, E.M., J.W. Mills, and B.A. Stanton. 1994. Actin-based cytoskeleton regulates a chloride channel and cell volume in a renal cortical collecting duct cell line. *J. Biol. Chem.* 269:7081–7089.

Schwiebert, E.K., M.E. Egan, T.-H. Hwang, S.B. Fulmer, S.S. Allen, G.R. Cutting, and W.B. Guggino. 1995. CFTR regulates outwardly rectifying chloride channels through an autocrine mechanism involving ATP. *Cell.* 81:1063–1073.

Silinsky, E.M. 1975. On the association between transmitter secretion and the release of adenine nucleotides from mammalian motor nerve terminals. *J. Physiol.* 247:145–162.

Sprague, R.S., M.L. Ellsworth, A.H. Stephenson, M.E. Kleinhenz, and A.J. Lonigro. 1998. Deformation-induced ATP release from red blood cells requires CFTR activity. *Am. J. Physiol.* 275:H1726–H1732.

Steinacker, P., L.A. Awni, S. Becker, T. Cole, S. Reymann, D. Hesse, H.D. Kratzin, C. Morris-Wortmann, C. Schwarzer, F.P. Thinnes, and N. Hilschmann. 2000. The plasma membrane of *Xenopus laevis* oocytes contains voltage-dependent anion-selective porin channels. *Int. J. Biochem. Cell Biol.* 32:225–234.

Strange, K., F. Emma, and P.S. Jackson. 1996. Cellular and molecular physiology of volume-sensitive anion channels. *Am. J. Physiol.* 270:C711–C730.

Sugita, M., Y. Yue, and J.K. Foskett. 1998. CFTR Cl^- channel and CFTR-associated ATP channel: distinct pores regulated by common gates. *EMBO J.* 17:898–908.

Sun, X.P., S. Supplisson, R. Torres, G. Sachs, and E. Mayer. 1992. Characterization of large-conductance chloride channels in rabbit colonic smooth muscle. *J. Physiol.* 448:355–382.

Sun, X.P., S. Supplisson, and E. Mayer. 1993. Chloride channels in myocytes from rabbit colon are regulated by a pertussis toxin-sensitive G protein. *Am. J. Physiol.* 264:G774–G785.

Takahashi, T., K. Matsushita, M.J. Welsh, and J.S. Stokes. 1994. Effect of cAMP on intracellular and extracellular ATP content of Cl^--secreting epithelia and 3T3 fibroblasts. *J. Biol. Chem.* 269: 17853–17857.

Taylor, A.L., B.A. Kudlow, K.L. Marrs, D.C. Gruenert, W.B. Guggino, and E.M. Schwiebert. 1998. Bioluminescence detection of ATP release mechanisms in epithelia. *Am. J. Physiol.* 275:C1391–C1406.

Thinnes, F.P., H. Götz, H. Kayser, R. Benz, W.E. Schmidt, H.D. Kratzin, and N. Hilshmann. 1989. Zur kenntnis der porine des menschen. I. Reinigung eines porins aus menschlichen B-lymphozyten (Porin 31HL) und sein topochemischer nachweis auf dem plasmalemm der herkunftszelle. *Biol. Chem. Hoppe-Seyler.* 370:11253–11264.

Vennekens, R., D. Trouet, A. Vankeerberghen, T. Voets, H. Cuppens, J. Eggermont, J.J. Cassiman, G. Droogmans, and B. Nilius. 1999. Inhibition of volume-regulated anion channels by expression of the cystic fibrosis transmembrane conductance regulator. *J. Physiol.* 515:75–85.

Wang, Y., R. Roman, S.D. Lidofsky, and J.G. Fitz. 1996. Autocrine signaling through ATP release represents a novel mechanism for cell volume regulation. *Proc. Natl. Acad. Sci. USA.* 93:12020–12025.

Watt, W.C., E.R. Lazarowski, and R.C. Boucher. 1998. Cystic fibrosis transmembrane regulator-independent release of ATP. Its implications for the regulation of $P2Y_2$ receptors in airway epithelia. *J. Biol. Chem.* 273:14053–14058.

Wunder, U.R., and M. Colombini. 1991. Patch clamping VDAC in liposomes containing whole mitochondrial membranes. *J. Membr. Biol.* 123:83–91.

Zimmermann, H. 1994. Signaling via ATP in the nervous system. *Trends Neurosci.* 17:420–426.